

## Abstract

Density functional theory (DFT) is nowadays the workhorse for simulating the electronic and geometric structure of real materials. Forces, i.e., the derivatives of the DFT total energy with respect to atomic positions, are indispensable for relaxing the atomic structure to its ground state. Accurate forces, moreover, enable the calculation of phonon spectra using the finite displacement method and of subsequent quantities such as electron- and magnon-phonon interaction.

We analyze the accuracy of the force computed within the all-electron full-potential linearized augmented plane-wave (FLAPW) method as realized in the FLEUR[1] code according to the formalism of Yu *et al.*[2]. As one criterion for the accuracy we employ the drift-force, i.e., the sum of all atomic forces in the unit cell, which should strictly vanish. Another criterion is the quality of the symmetry of the force-constant matrix. We show that both criteria can be fulfilled to an accuracy of  $1\mu\text{Htr}/a_B$  only if (a) the core-electron tails are properly taken into account and (b) a large angular momentum cut-off is applied. We propose a refined formulation of the force that cures the aforementioned demands on the LAPW setup to a great extent. As an example, we present results on MgO and EuTiO<sub>3</sub>.

## The FLAPW method

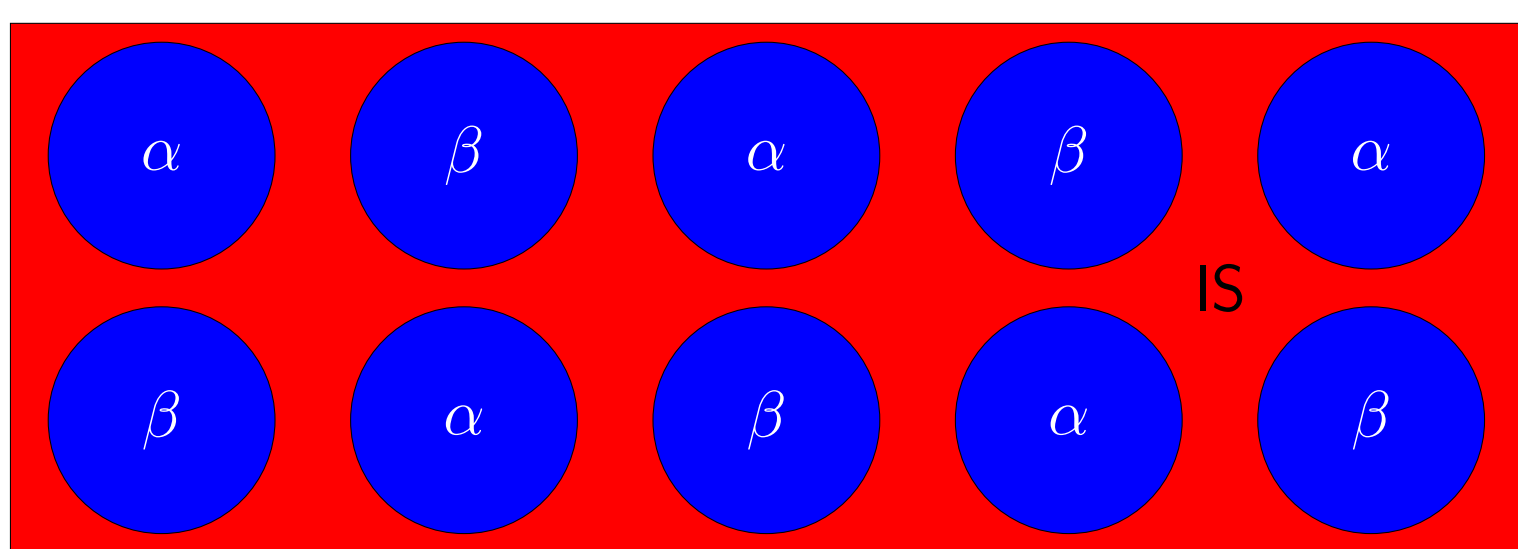


Figure 1: Partitioning of crystal volume into interstitial and muffin-tin spheres.

- space is partitioned into muffin-tin (MT) spheres centered at the atomic positions  $\tau_\alpha$  and the remaining interstitial region (IS)
- linearized augmented plane-waves are used for representing the valence-electron wave functions ( $\mathbf{r}_\alpha = \mathbf{r} - \tau_\alpha$ )

$$\phi_{\mathbf{k}\mathbf{G}}(\mathbf{r}) = \begin{cases} \frac{1}{\sqrt{\Omega}} e^{i(\mathbf{k}+\mathbf{G})\cdot\mathbf{r}} & , \mathbf{r} \in \text{IS} \\ \sum_L^{\ell_{\max}} R_{\alpha,L}^{\mathbf{k}\mathbf{G}}(r_\alpha, E_\ell^\alpha) Y_L(\hat{\mathbf{r}}_\alpha) & , \mathbf{r} \in \text{MT}_\alpha \end{cases} \quad (1)$$

where the radial functions  $R_{\alpha,L}^{\mathbf{k}\mathbf{G}}$  are linear combinations of solutions  $\varphi_\ell(r_\alpha, E_\ell^\alpha)$  to the radial Schrödinger equation and their energy derivatives  $\dot{\varphi}_\ell(r_\alpha, E_\ell^\alpha)$ ; the expansion coefficients are determined by a matching to the interstitial plane-wave up to first order

- fully-relativistic Dirac equation with the spherical crystal potential is solved on an extended radial mesh for the core states
- dual representation is employed for density and potential

$$f(\mathbf{r}) = \begin{cases} \sum_{\mathbf{G}}^{\geq 2G_{\max}} \hat{f}(\mathbf{G}) e^{i\mathbf{G}\cdot\mathbf{r}} & , \mathbf{r} \in \text{IS} \\ \sum_L^{\geq 2\ell_{\max}} f_L^\alpha(r_\alpha) Y_L(\hat{\mathbf{r}}_\alpha) & , \mathbf{r} \in \text{MT}_\alpha \end{cases} \quad (2)$$

## Force and Force-Constant Matrix

In equilibrium and for small atomic displacements  $\mathbf{u}$  the total energy obeys (within the harmonic regime):

$$E_{\text{tot}}(\mathbf{u}) = E_{\text{tot}}(0) + \frac{1}{2} \sum_{\alpha,i,\beta,j} \Phi_{\alpha,i,\beta,j} u_{\alpha,i} u_{\beta,j} \quad (3)$$

The force  $-\nabla_{\mathbf{u}_\alpha} E_{\text{tot}}$  on atom  $\alpha$  is thus directly proportional to the displacement

$$\mathbf{F}_\alpha = -\nabla_{\mathbf{u}_\alpha} E_{\text{tot}}(\mathbf{u}) = -\sum_\beta \Phi_{\alpha,\beta} \cdot \mathbf{u}_\beta, \quad (4)$$

where  $\Phi$  denotes the force-constant matrix (FCM). According to Young's theorem it is symmetric:

$$\Phi_{\alpha,i,\beta,j} = \frac{\partial^2 E_{\text{tot}}(\mathbf{u})}{\partial u_{\alpha,i} \partial u_{\beta,j}} = \frac{\partial^2 E_{\text{tot}}(\mathbf{u})}{\partial u_{\beta,j} \partial u_{\alpha,i}} = \Phi_{\beta,j,\alpha,i} \quad (5)$$

Translational invariance implies the acoustic-sum rule, i.e.  $\sum_\alpha \mathbf{F}_\alpha = 0$ . If this sum does not vanish, the resulting value is called drift force.

## Forces in FLAPW

Forces in the FLAPW method are formulated by Soler and Williams[3] and Yu *et al.* We focus on the latter formulation as it is implemented in FLEUR. In addition to the Hellman-Feynman force so-called Pulay forces[4] occur in the FLAPW approach. They arise from the position dependence of the LAPW basis functions:

$$\mathbf{F}_{\text{tot}}^\alpha = \mathbf{F}_{\text{HF}}^\alpha + \mathbf{F}_{\text{core}}^\alpha + \mathbf{F}_{\text{val}}^\alpha + \mathbf{F}_{\text{disc}}^\alpha \quad (6)$$

$$\mathbf{F}_{\text{HF}}^\alpha = Z_\alpha \nabla_{\tau_\alpha} \left\{ \int_{\mathbb{R}^3} \frac{\rho(\mathbf{r})}{|\tau_\alpha - \mathbf{r}|} d^3\mathbf{r} - \sum_\beta \sum_{\mathbf{R}} \frac{Z_\beta}{|\tau_\alpha - \tau_\beta + \mathbf{R}|} \right\} \quad (7)$$

$$\mathbf{F}_{\text{core}}^\alpha = - \int_{\text{MT}_\alpha} \rho_{\text{core}}^\alpha(\mathbf{r}) \nabla V_{\text{eff}}(\mathbf{r}) d^3\mathbf{r} \quad (8)$$

$$\mathbf{F}_{\text{val}}^\alpha = -2 \sum_{ik} n_{ik} \text{Re} \left\langle \frac{\delta \psi_{ik}}{\delta \tau_\alpha} \left| \mathcal{H} - \epsilon_{ik} \right| \psi_{ik} \right\rangle \quad (9)$$

$$\mathbf{F}_{\text{disc}}^\alpha = \frac{1}{2} \sum_{ik} n_{ik} \oint_{\partial \text{MT}_\alpha} \mathbf{n} \left\{ \psi_{ik}^*(\mathbf{r}) \nabla^2 \psi_{ik}(\mathbf{r}) \right\} \Big|_{\text{MT}_\alpha - \text{IS}} dS \quad (10)$$

The corrections are due to:

- $\mathbf{F}_{\text{core}}^\alpha$ : atomic position changes, hence core states feel displaced potential. (Core states assumed to vanish at muffin-tin sphere boundary.)
- $\mathbf{F}_{\text{val}}^\alpha$ : valence states depend on atomic position through the matching coefficients and the radial functions in the muffin-tin spheres.
- $\mathbf{F}_{\text{disc}}^\alpha$ : muffin-tin part of basis only matched up to first order at muffin-tin boundary, discontinuous in second order. (After applying the Laplacian, the interstitial part is evaluated using the muffin-tin basis.)

## Refined Forces

With the force implementation according to Yu *et al.* we found that the acoustic sum rule and the symmetry of the FCM are only fulfilled to the order of  $0.1m\text{Htr}/a_B$  (see Results for MgO and EuTiO<sub>3</sub>). To reliably calculate phonon spectra using the finite-displacement approach[5–7], a higher accuracy is vital. Hence, we refined the force formulation according to Yu *et al.* at three points:

- a) The restriction of the integral to the MT sphere in Eq. (9) is given by:

$$\mathbf{F}_{\text{core}}^\alpha = - \int_{\text{MT}_\alpha} \rho_{\text{core}}^\alpha(\mathbf{r}) \nabla V_{\text{eff}}(\mathbf{r}) d^3\mathbf{r} \quad (11)$$

This is necessary as high lying core states can leak out of their MT sphere as demonstrated for MgO below:

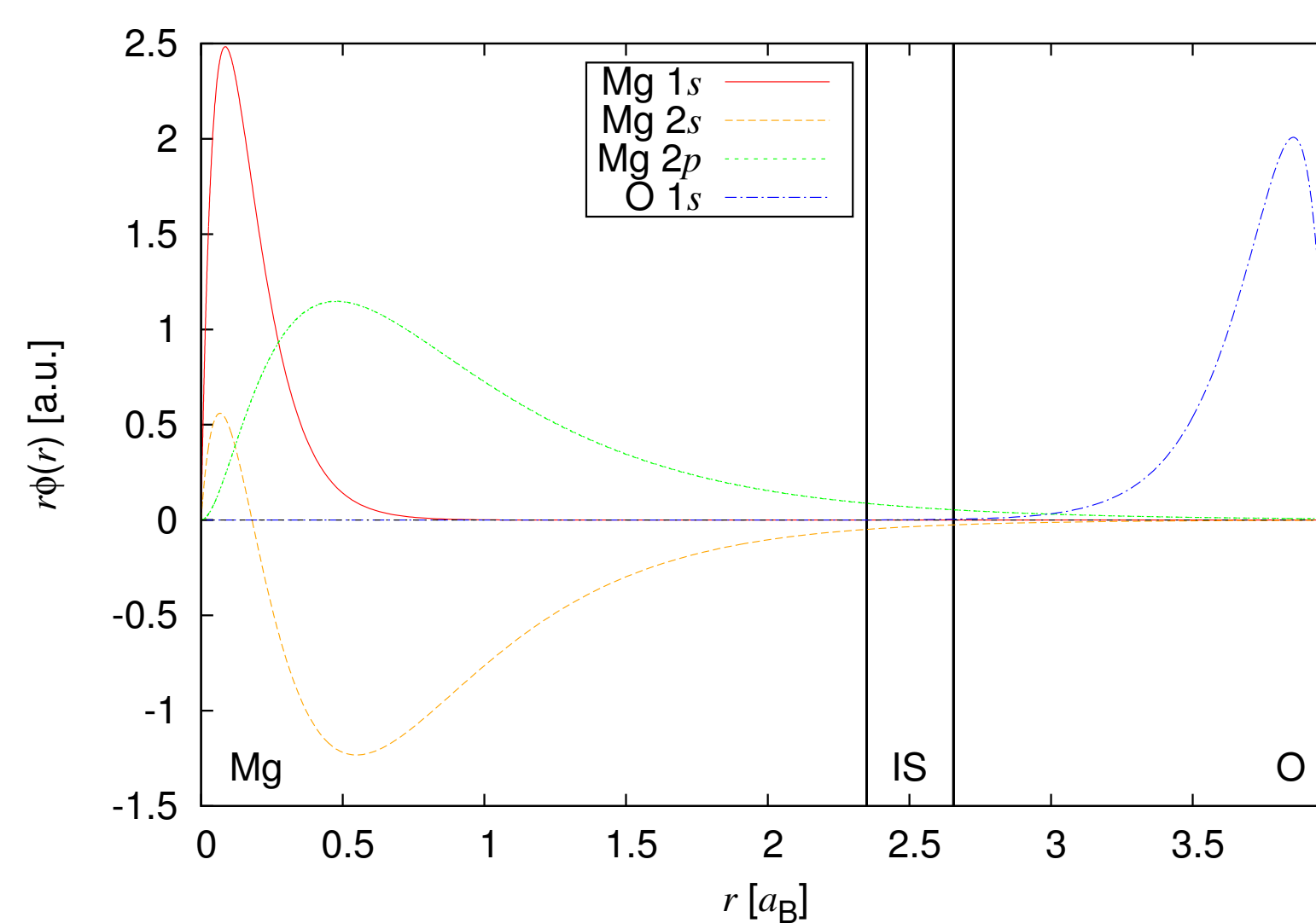


Figure 2: Core states of adjacent magnesium and oxygen atoms in MgO.

- b) We use the explicit representation of the IS wave function in Eq. (10). The integral is then evaluated by applying the Rayleigh expansion for the plane wave up to a large angular-momentum cutoff  $\ell_{\text{big}}$  (set to 60 in the examples below):

$$\phi_{\mathbf{k}\mathbf{G}}(\mathbf{R}_\alpha + \tau_\alpha) \Big|_{\text{IS}} \approx \frac{4\pi}{\sqrt{\Omega}} e^{i\mathbf{k}\cdot(\mathbf{R}_\alpha + \tau_\alpha)} e^{i\mathbf{G}\cdot\tau_\alpha} \sum_L^{\ell_{\text{big}}} i^\ell Y_L^*(\hat{\mathbf{G}}) j_\ell(GR_\alpha) Y_L(\hat{\mathbf{r}}_\alpha) \quad (12)$$

- c) In addition to the force contributions Eq. (8)-(10) we propose an additional term, which arises from the discontinuity of the potential and density at the MT sphere boundary:

$$\mathbf{F}_{\text{surf}}^\alpha = - \oint_{\partial \text{MT}_\alpha} \hat{\mathbf{n}} \left[ \rho(\mathbf{r}) (V_{\text{Coul}}(\mathbf{r}) + \epsilon_{\text{xc}}(\mathbf{r})) \Big|_{\text{MT}_\alpha} - \rho(\mathbf{r}) (V_{\text{Coul}}(\mathbf{r}) + \epsilon_{\text{xc}}(\mathbf{r})) \Big|_{\text{IS}} \right] dS \quad (13)$$

The IS part is treated using the Rayleigh expansion up to  $\ell_{\text{big}}$  as in b).

We note that we still stick to the frozen-augmentation approximation, i.e. the variation of the MT radial functions beyond the gradient w.r.t. atomic position is neglected.

## Results on MgO

For fcc MgO with a lattice constant of  $7.970a_B$  we displaced the magnesium sublattice by  $0.199a_B$  against the oxygen sublattice and analyzed the drift term and the symmetry of the force constant matrix. We also conducted calculations using local orbitals for the 2s and 2p states of Mg.

### Drift Force

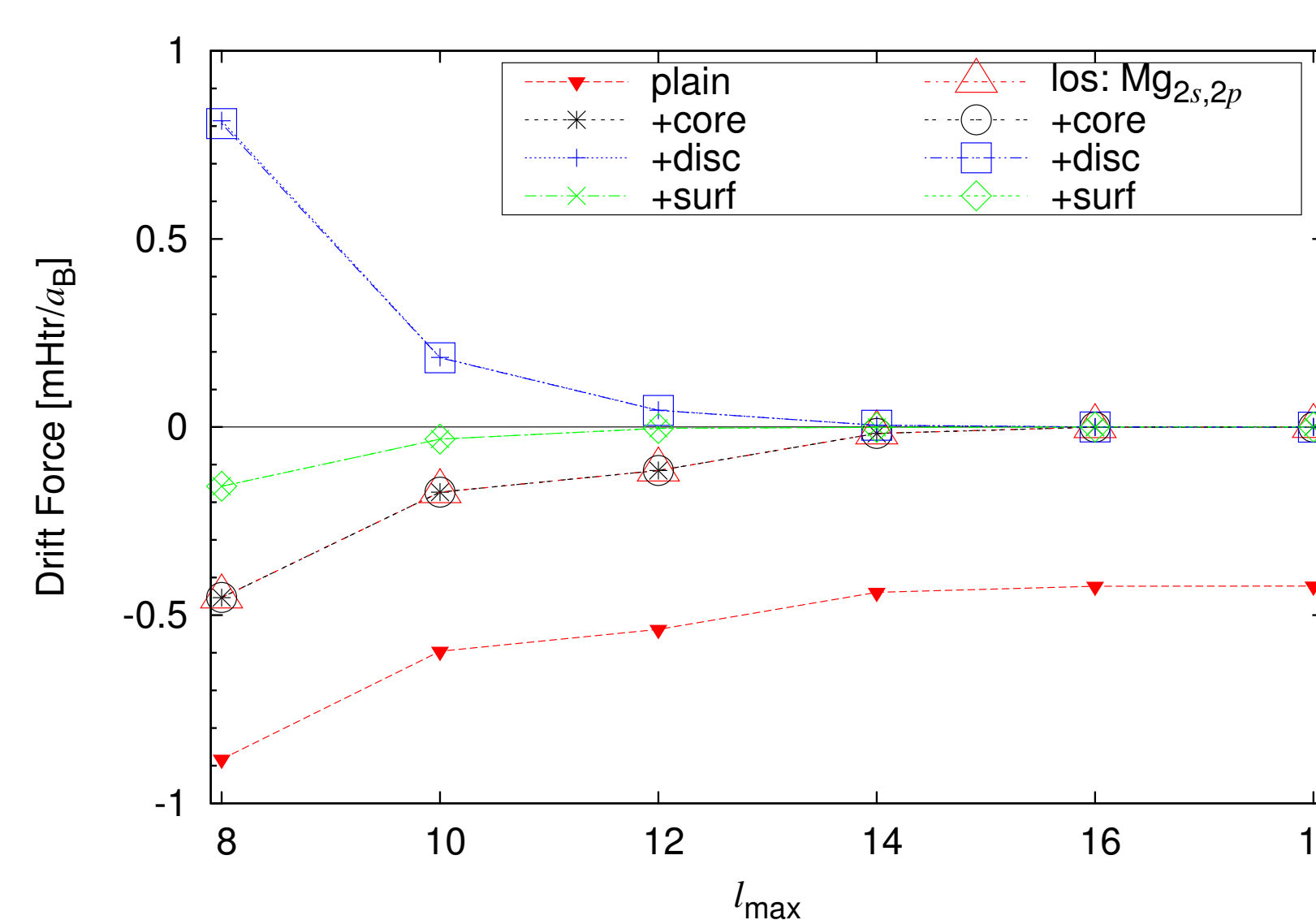


Figure 3: Drift forces w.r.t.  $\ell_{\max}$ -cutoff in MgO.

- Eq. (11) shifts the asymptote of the drift force to zero, making it convergible w.r.t. the angular-momentum cutoff.
- Eq. (12) is a massive change in drift force for small  $\ell_{\max}$ , where the discontinuity in the basis functions is strongest.
- Eq. (13) compensates for the massive change and yields the best convergence behavior.
- Treating leaking core states by local orbitals has the same effect on the drift term as evaluating the core correction over the whole unit-cell.

### Force-Constant Matrix

	plain		+core,+disc,+surf	
force on \ disp	Mg	O	Mg	O
Mg	-11.6046	11.6046	-11.1655	11.1655
O	11.1652	-11.1652	11.1649	-11.1649
drift	<b>-0.4394</b>	<b>0.4394</b>	<b>-0.0006</b>	<b>0.0006</b>
los: Mg <sub>2s,2p</sub>				
Mg	-10.8027	10.8027	-10.7861	10.7861
O	10.7857	-10.7857	10.7854	-10.7854
drift	-0.0170	0.0170	-0.0007	0.0007

Table 1: Part of force matrix of MgO with and without local orbitals.  $\ell_{\max}$ -cutoff is 14. Forces are given in  $m\text{Htr}/a_B$ .

- In the case that the Mg 2s and 2p states are treated as core electrons the x-component of the force matrix exhibits an improved symmetry by three orders of magnitude.
- A substantial improvement of the symmetry is even present if the Mg 2s and 2p states are described with local orbitals.

## Results on EuTiO<sub>3</sub>

For the perovskite EuTiO<sub>3</sub> with a lattice constant of  $7.370a_B$  we displaced each atom by  $0.022a_B$  along x-direction in a separate calculation each and analyzed the drift term and the symmetry of the force constant matrix. The 5s and 5p states of europium and the 3p states of titanium are treated as local orbitals.

### Drift Force

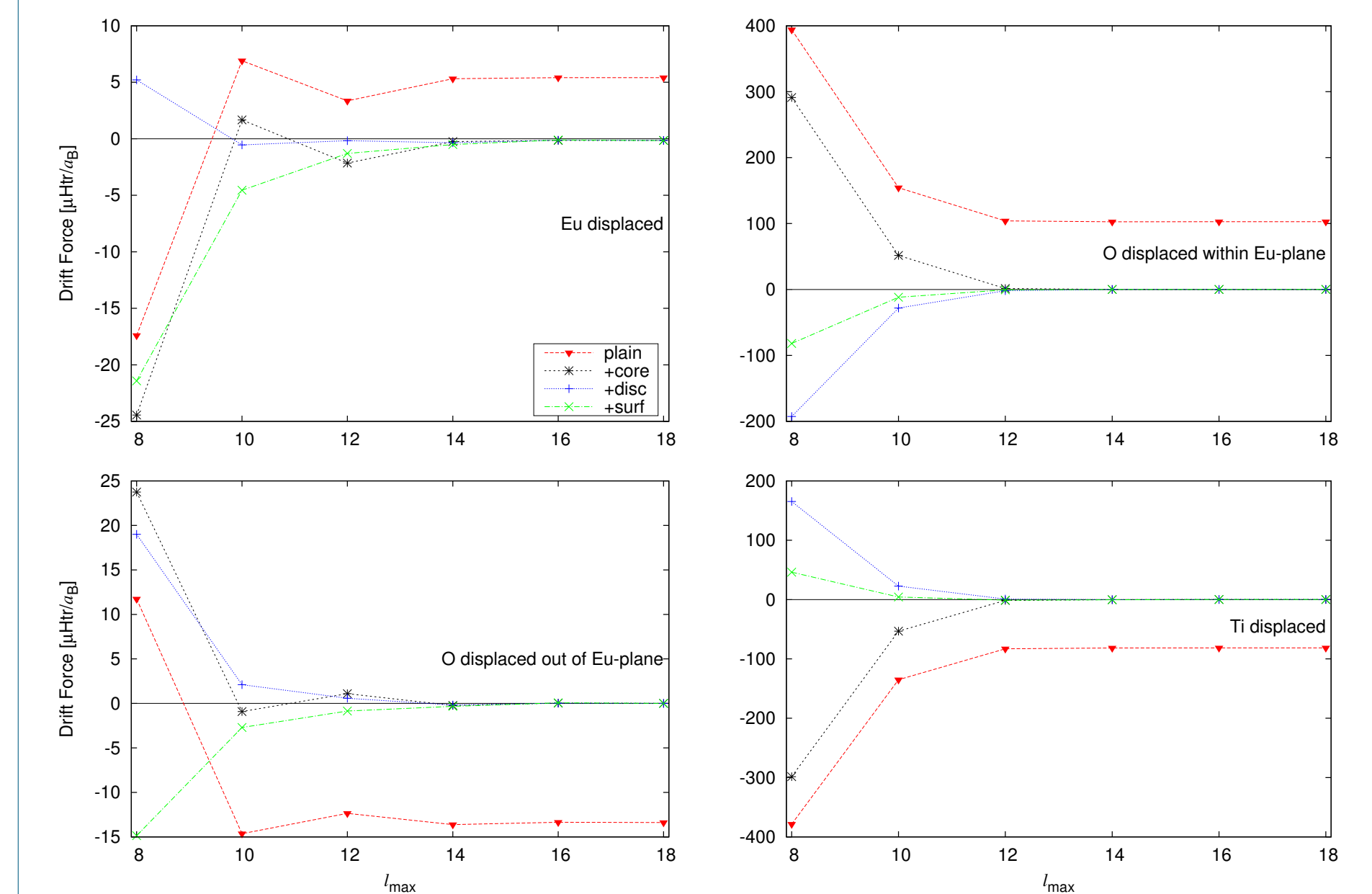


Figure 4: Drift forces w.r.t.  $\ell_{\max}$ -cutoff in EuTiO<sub>3</sub>.

- Eq. (11) shifts the asymptote of the drift force to zero again.
- Eq. (12) is a significant contribution for small  $\ell_{\max}$  at all calculations apart from when oxygen is displaced out of the europium plane.
- Eq. (13) compensates again and yields good convergence behavior apart from when europium is displaced.

The force scale on the two subfigures to the left is such however, that any correction produces drift forces within the target margin of  $1\mu\text{Htr}/a_B$  per atom starting from  $\ell_{\max} = 10$ .

### Force-Constant Matrix

	Eu	O <sub>0 1/2</sub>	O <sub>3/2 0</sub>	O <sub>3/2 0</sub>	Ti
Eu <sub>000</sub>	-274.373	198.968	-273.033	-273.033	621.304
O <sub>0 1/2</sub>	200.293	-3209.879	1067.026	1067.026	<b>879.805</b>
O <sub>3/2 0</sub>	-274.634	1065.862	-831.746	-194.171	233.028
O <sub>1 1/2 0</sub>	-274.634	1065.862	-194.171	-831.746	233.028
Ti <sub>1 1/2 2/2</sub>	626.706	<b>983.271</b>	219.577	219.577	-2050.128
drift	3.358	104.084	-12.347	-12.347	-82.963
maximal deviation:			<b>103.466 ± 20.693 per atom</b>		
	Eu	O <sub>0 1/2</sub>	O <sub>3/2 0</sub>	O <sub>3/2 0</sub>	Ti
Eu <sub>000</sub>	-272.207	199.179	-274.259	-274.259	621.288
O <sub>0 1/2</sub>	200.295	-3209.809	1067.024	1067.024	<b>879.737</b>
O <sub>3/2 0</sub>	-274.642	1065.860	-831.748	-194.171	233.039
O <sub>1 1/2 0</sub>	-274.642	1065.860	-194.171	-831.748	233.039
Ti <sub>1 1/2 2/2</sub>	619.899	<b>878.328</b>	232.300	232.300	-1967.990
drift	-1.297	-0.582	-0.854	-0.854	-0.887
maximal deviation:			<b>1.409 ± 0.282 per atom</b>		

Table 2: Part of the force matrix of EuTiO<sub>3</sub> with no and all additional terms used. Each row corresponds to one atom displaced, each line to the atom the force acts upon.  $\ell_{\max}$ -cutoff is 12 for all atom types. Forces are given in  $\mu\text{Htr}/a_B$ .

- The x-component of the force matrix exhibits an improved symmetry by two orders of magnitude.
- Entries changing most are related to moving oxygen towards titanium or vice versa. Reducing the distance between these atoms increases the weight of the electron partially lost from Ti in the oxygen muffin-tin.

## Setup Details

- A  $10 \times 10 \times 10$  sampling of the Brillouin zone is used in both examples
- All atoms within a calculation use the same  $\ell_{\max}$ -cutoff
- The LDA xc-functional of Vosko, Wilk, and Nusair is employed
- MgO:  $k_{\max} = 5.5a_B^{-1}$ ,  $R_{\text{Mg}} = 2.35a_B$ ,  $R_{\text{O}} = 1.33a_B$
- ETO:  $k_{\max} = 4.8a_B^{-1}$ ,  $R_{\text{Eu}} = 2.60a_B$ ,  $R_{\text{O}} = 1.41a_B$ ,  $R_{\text{Ti}} = 2.21a_B$

## Conclusions and Outlook

- Based on the force formulation of Yu *et al.* we proposed a refined scheme for calculating forces within the FLAPW method.
- We demonstrated that this refined scheme leads to a vanishing drift term ( $\rightarrow$  acoustic sum rule) and an improved symmetry of the FCM.
- The new formalism is less sensitive to the treatment of semicore states and only affects the force calculation step, not the SCF cycle.
- In the perspective of phonon calculations based on the finite-displacement approach, a rigorous treatment of the atomic force results in a diminished need to artificially impose the acoustic sum rule and the symmetry of the FCM. In this way, phonon spectra become more reliable.

## Acknowledgments

We thank Konstantin Rushchanskii and Gustav Bihlmyer for insightful discussions.

## References

- [1] <http://www.flapw.de>
- [2] R. Yu, D. Singh, and H. Krakauer, Phys. Rev. B **43** (1991), 6411–6422
- [3] J. M. Soler and A. R. Williams, Phys. Rev. B **40** (1989), 1560–1564
- [4] P. Pulay, Molecular Physics **17** (1969), 197–204
- [5] K. Parlinski, Z. Q. Li, and Y. Kawazoe, Phys. Rev. Lett. **78** (1997), 4063–4066
- [6] D. Alfè, G. D. Price, and M. J. Gillan, Phys. Rev. B **64** (2001), 045123
- [7] G. Kresse, J. Furthmüller, and J. Hafner, EPL (Europhysics Letters) **32** (1995), 729